

## Thermal Performance Evaluation of PLUS-7 Fuel Assembly

**J. T. Kwon, K. Y. Nahm, J. S. Lim and C. O. Park**

KEPCO Nuclear Fuel Co.

P. O. Box 14, Yusung, Daejeon, Korea, 305-600

jtkwon@mail.knfc.co.kr

### ABSTRACT

The PLUS-7 fuel has been developed with mixing vane grids for the Korean Standard Nuclear Plants. Critical Heat Flux (CHF) tests were performed to determine thermal performance for the PLUS-7 fuel at Heat Transfer Research Facility of Columbia University. The KCE-1 CHF correlation has been developed based on the test data. The functional form of the KCE-1 correlation is the same as the CE-1 CHF correlation which has been used for thermal design of KSNPs. The thermal performance of PLUS-7 fuel is evaluated by comparing the corresponding CHF data for the current KSNP Standard fuel which has no mixing vanes. The increase in the hot rod average heat flux of PLUS-7 fuel was evaluated to be 12.8%, in average, at the same inlet conditions.

### 1. INTRODUCTION

The PLUS-7 fuel has been developed with mixing vane grids for the Korean Standard Nuclear Plants (KSNP) of which 5 units are in operation and 3 are under construction. Besides the mixing vane grid, the PLUS-7 features include: Removable Top Nozzle, Reduced Rod Bow Inconel top grid, ZIRLO™ mid-grids, high burnup Inconel bottom grid, Debris Filter Bottom Nozzle and ZIRLO™ guide thimbles and fuel claddings. The PLUS-7 is a 16x16 assembly having a 150.0 inches fuel stack length. The assembly contains clad fuel rods that are 0.374 inches outer diameter. The structural skeleton is comprised of four guide thimbles of 0.980 inches outer diameter and one center instrumentation tube. Beginning at the lower end of the assembly, there is a vaneless Inconel 718 structural end grid. A vaneless nonstructural Inconel 718 debris protective grid is utilized next. Nine ZIRLO™ mid-grids with mixing vanes are utilized next, followed at the very top of the assembly by an Inconel 718 vaneless structural end grid.

The PLUS-7 mid-grid design includes contoured grid spring and dimple, diamond shape of spring ligament and horizontal spring, closed spring windows and increased strap (Figure 1). The contoured spring and dimple are introduced to increase the fuel rod contact area and to decrease the contact stress for better fretting wear behavior. The diamond shape of spring ligament and horizontal spring will improve flow balance with the balanced vane pattern. The increased strap height improves load-bearing capability to meet the high crush strength requirement for application on high seismic plant. The mixing vane improves heat transfer between coolant and fuel rod and increases thermal margin. Therefore, the thermal performance of a fuel highly depends on the spacer grid design.

Critical Heat Flux (CHF) tests were performed to determine the thermal performance for the PLUS-7 fuel at Heat Transfer Research Facility of Columbia University[1, 2]. The KCE-1 correlation, whose functional form is the same as the CE-1 CHF correlation[3] which has been used for thermal design of KSNPs, is developed based on the CHF data obtained. The thermal performance of PLUS-7 fuel is evaluated by comparing the corresponding CHF data for the current KSNP Standard fuel which has no mixing vanes. The predicted CHF's from each correlation are compared at a variety of core inlet conditions.

## 2. DEVELOPMENT OF CHF CORRELATION

### 2.1 CHF Test Data

The tests simulated 6x6 arrays of the fuel assembly geometry with and without guide tube (Figures 2 and 3), mixing vane mid-grids, non-uniform radial power distribution, 1.475 chopped cosine axial power distribution, heated length of 150 inches and grid spacing of 15.7 inches (Table 1).

The CHF data cover the following parameter ranges:

Pressure	1400 to 2490 psia
Mass velocity	0.90 to 3.70x10 <sup>6</sup> lbm/hr-ft <sup>2</sup>
Inlet temperature	250 to 637 deg. F

Total 219 CHF data were obtained from both of test assemblies.

### 2.2 CHF Correlation Development

The functional form of the KCE-1 correlation is the same as the CE-1 correlation, which has been used for the thermal design of KSNP. The CE-1 correlation has the following form:

$$q_{CHF,U}'' = \frac{B_1 (d/d_m)^{B_2} [(B_3 + B_4 P)(G/10^6)^{(B_5+B_6)} - (G/10^6) \chi h_{fg}]}{(G/10^6)^{(B_7 P + B_8 (G/10^6))}}$$

where	$q_{CHF,U}''$	critical heat flux for uniform axial power, <i>MBtu/hr-ft<sup>2</sup></i>
	$P$	pressure, <i>psia</i>
	$d$	heated diameter of subchannel, <i>inches</i>
	$d_m$	heated diameter of matrix subchannel, <i>inches</i>
	$G$	local mass velocity at CHF location, <i>lbm / hr-ft<sup>2</sup></i>
	$\chi$	local coolant quality at CHF location, decimal fraction
	$h_{fg}$	latent heat of vaporization, <i>Btu/lbm</i> .

The CE-1 CHF correlation was developed with uniform axial power distribution data[3]. The correlation underpredicts the CHF for non-uniform axial power distribution when it is combined with the non-uniform shape F-factor[4, 5]. Like the current application of CE-1 CHF correlation to KSNP fuel, the application of the KCE-1 CHF correlation to the PLUS-7 fuel design will also be conservative when the correlation is convoluted with the F-factor for non-uniform axial power shapes.

The CHF data are evaluated by using the TORC code[6], which is an adoption of the COBRA III C code. The TORC code is a steady state thermal hydraulic code that solves the three-dimensional lateral mass, momentum and energy equations in an open channel reactor. The local fluid conditions at the measured CHF locations are extracted to get the first cut for the development of the KCE-1 CHF correlation. The coefficients of KCE-1 CHF correlation are developed by an iterative process for the correlation optimization. A plot of the measured to predicted CHF for all data points is shown in Figure 4. Scatter plots of the ratio of measured to predicted CHF versus pressure, mass velocity and quality are shown in Figures 5 through 7, respectively. As shown in the Figures, the ratios of measured to predicted CHF(M/P) are evenly distributed around the line of M/P equals 1, even though there are some deviations in the low pressure region of Figure 5.

### 3. EVALUATION OF THERMAL PERFORMANCE

#### 3.1 Comparison of CHF Power

The increase in CHF power between PLUS-7 and KSNP Standard fuels is estimated. To quantify this margin, CHF Test 59[7] was chosen as representative of KSNP Standard fuel because of the below reasons:

- Same rod diameter
- Same rod pitch
- Same heated length
- Same 2x2 thimble tube
- Similar grid span
- Similar axial power shape (1.47 versus 1.475 peak cosine)

In the test matrix 1010[1], 36 points were chosen to match data in test 59. The acceptance criteria for deviations of the CHF loop parameters from the matching points of Test 59 is as follows:

- Exit pressure: +/- 25 psi
- Inlet temperature: +/- 2.5 °F
- Mass velocity: +/- 0.05 Mlb/hr-ft<sup>2</sup>

The overpower margin for each matching point is calculated using the below equation:

$$\delta = \frac{(q_{PLUS-7} - q_{Test59})}{q_{Test59}}$$

The average overpower increase for all matching pairs are calculated using all matched pair data:

$$Avg \ \delta = \frac{1}{N} \sum_{i=1}^N \delta_i$$

where  $N$  number of all matched pairs  
 $q$  hot rod heat flux at DNB.

The increase in the hot rod average heat flux between PLUS-7 and KSNP Standard fuels was evaluated to be 12.8%. A plot showing the CHF power increase of PLUS-7 fuel is presented in Figure 8.

#### 3.2 Comparison of Predicted CHF's

A set of plots is generated to compare the predicted CHF from the KCE-1 and CE-1 CHF correlations at a variety of core inlet conditions using the TORC code (Figures 9 through 17). The CHF values are generated as a function of pressure, mass velocity and quality.

Based upon a review of the plots, a few points are worthy of mention. The CHF's from KCE-1 CHF correlation are improved considerably compared to those from CE-1 correlation for both of matrix and thimble tube corner subchannels. It is noted that the difference in the predicted CHF's in the matrix and thimble tube corner subchannels is smaller for the KCE-1 correlation. Considering that subchannel adjacent to the cold wall has lower CHF due to the cold wall effect[8, 9], this indicates

that the mixing effects of mixing vanes is larger for the thimble tube corner subchannels. This is also shown in several plots where the predicted CHF with the CE-1 correlation is close to, if not higher than, the predicted CHF with the KCE-1 correlation in the matrix subchannel, especially at low qualities.

#### 4. CONCLUSIONS

The PLUS-7 fuel has been developed with mixing vane grids for the Korean Standard Nuclear Plants. KCE-1 CHF correlation is developed based on the data from the CHF test performed to determine thermal performance of the PLUS-7 fuel.

The thermal performance of PLUS-7 fuel is evaluated by comparing the corresponding CHF data for the current KSNP Standard fuel which has no mixing vanes. The increase in the hot rod average heat flux of PLUS-7 fuel is evaluated to be 12.8%, in average, at the same inlet conditions.

The predicted CHF from KCE-1 CHF correlations are improved considerably compared those from CE-1 correlation. The mixing effect of mixing vanes is larger for the subchannels adjacent to the cold wall, that is, thimble tube.

#### REFERENCES

1. CU-HTRF-2001-W1010, "Critical Heat Flux Tests on PWR Fuel Assemblies for Westinghouse Electric Company Test No. 101.0", August 2001.
2. CU-HTRF-2001-W1020, "Critical Heat Flux Tests on PWR Fuel Assemblies for Westinghouse Electric Company Test No. 102.0", August 2001.
3. CENPD-162-P-A, "C-E Critical Heat Flux, Critical Heat Flux Correlation for C-E Fuel Assemblies with Standard Spacer Grids, Part 1 Uniform Axial Power Distribution", September 1976.
4. CENPD-207-P-A, "C-E Critical Heat Flux, Critical Heat Flux Correlation for C-E Fuel Assemblies with Standard Spacer Grids, Part 2 Nonuniform Axial Power Distribution", December 1984.
5. Tong, L. S., "Boiling Crisis and Critical Heat Flux", *U. S. Atomic Energy Commission*, 1972, pp. 54-55.
6. CENPD-161-P-A, "TORC Code, A Computer Code for Determining the Thermal Margin of a Reactor Core", April 1986.
7. CENPD-220-P, "1975 CHF Test Program", March 1976.
8. L. S. Tong, "Prediction of Departure from Nucleate Boiling for an Axially Non-Uniform Heat Flux Distribution", *J. of Nuclear Energy*, 1967 pp241 to 248.
9. L. S. Tong, "An Evaluation of the Departure from Nucleate Boiling in Bundles of Reactor Fuel Rods", *Nuclear Science and Engineering*, 33, 7-15(1968).

Table 1 Geometric Characteristics of CHF Tests for PLUS-7 Fuel

Test Class	Fuel Type	Rod Diam. ~ in.	Rod Pitch ~ in.	Heated Length ~ in.	Grid Spacing ~ in.	Guide Tube	GT Diam. ~ in.	Axial Shape	Grid Material
Typical	16x16	0.374	0.506	150.0	15.7	No	N/A	1.475 cos	ZIRLO™
Thimble	16x16	0.374	0.506	150.0	15.7	Yes	0.980	1.475 cos	ZIRLO™

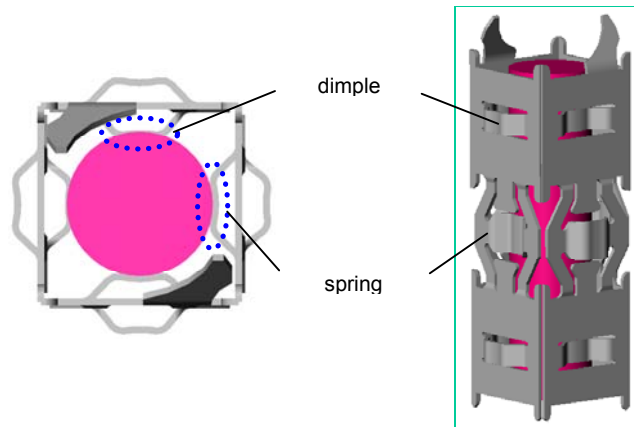


Figure 1 PLUS7 Fuel Assembly Mid-Grid Configuration

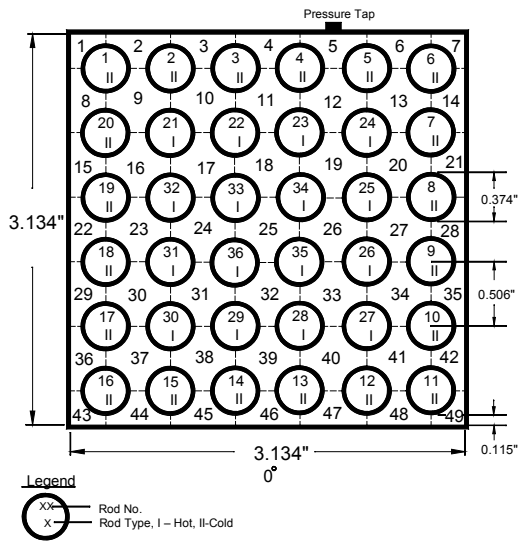


Figure 2 Typical Cell Test Assembly

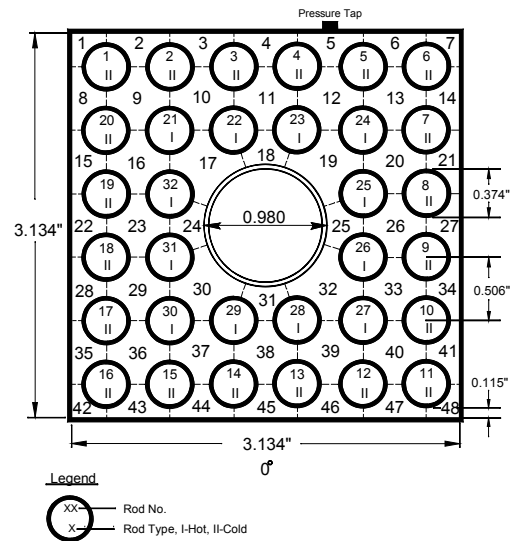


Figure 3 Thimble Cell Test Assembly

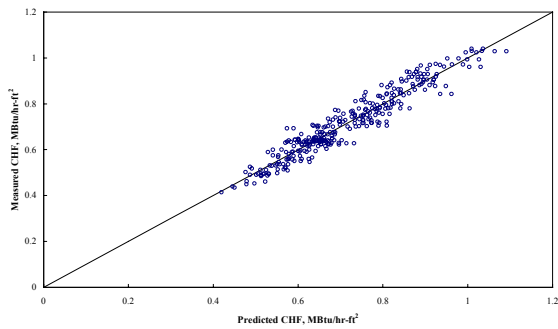


Figure 4 Measured to Predicted CHF for KCE-1 Correlation and Source Data

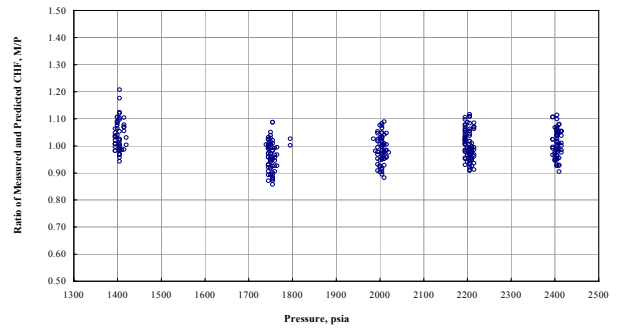


Figure 5 Ratio of Measured to Predicted CHF with Pressure for KCE-1 Correlation and Source Data

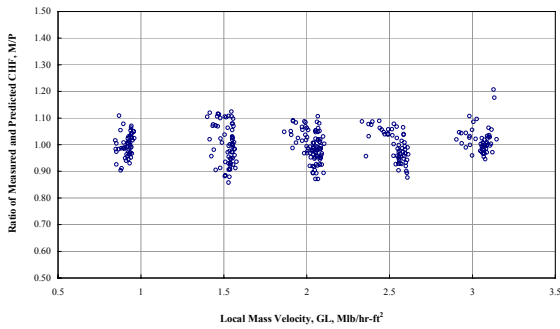


Figure 6 Ratio of Measured to Predicted CHF with Mass Velocity

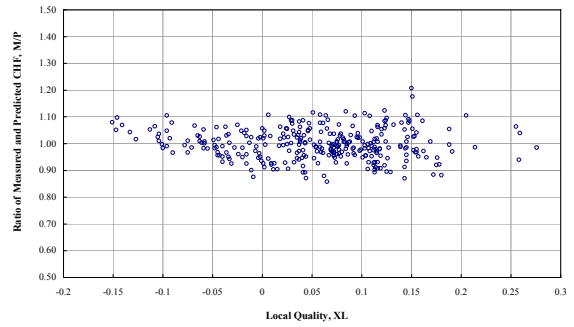


Figure 7 Ratio of Measured to Predicted CHF with Quality

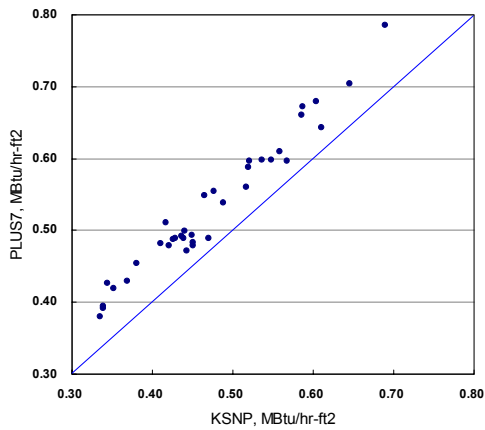


Figure 8 Comparison of Hot Rod Power at DNB

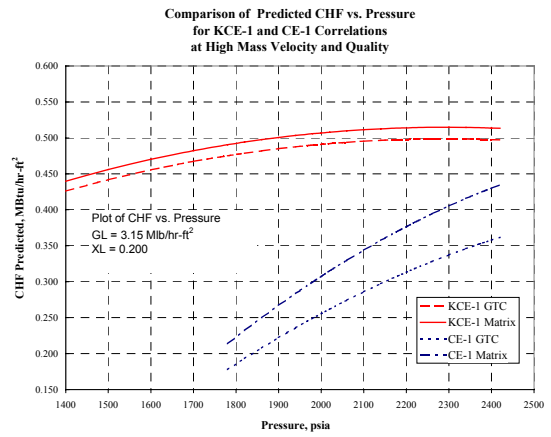


Figure 9 Predicted CHF vs. Pressure at High Mass Velocity & Quality

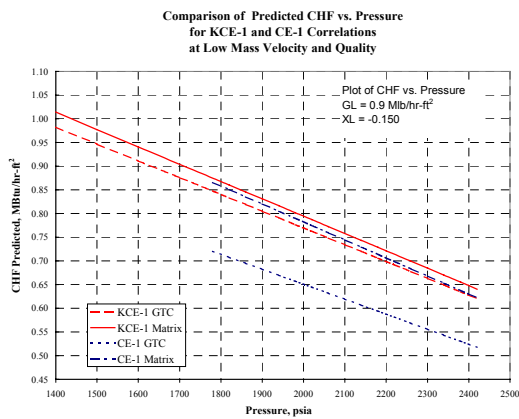


Figure 10 Predicted CHF vs. Pressure at Low Mass Velocity & Quality

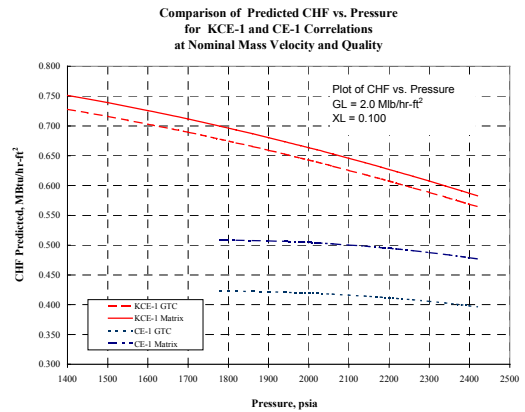


Figure 11 Predicted CHF vs. Pressure at Nominal Mass Velocity & Quality

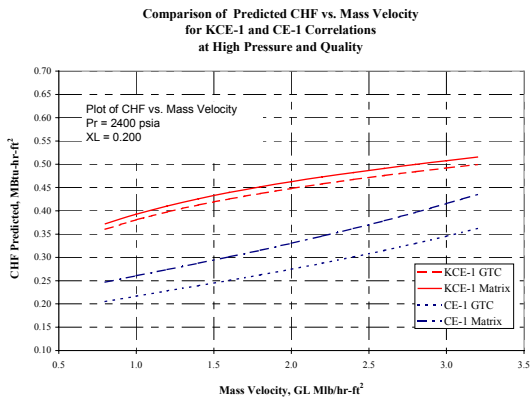


Figure 12 Predicted CHF vs. Mass Velocity at High Pressure & Quality

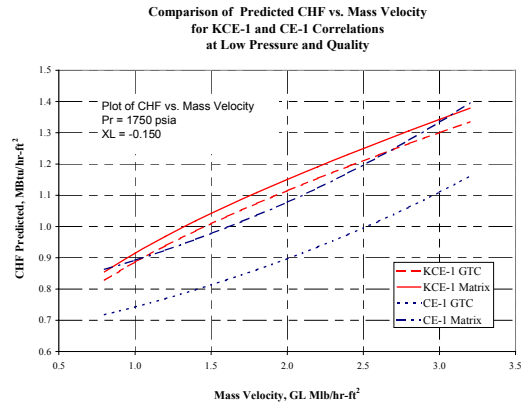


Figure 13 Predicted CHF vs. Mass Velocity at Low Pressure & Quality

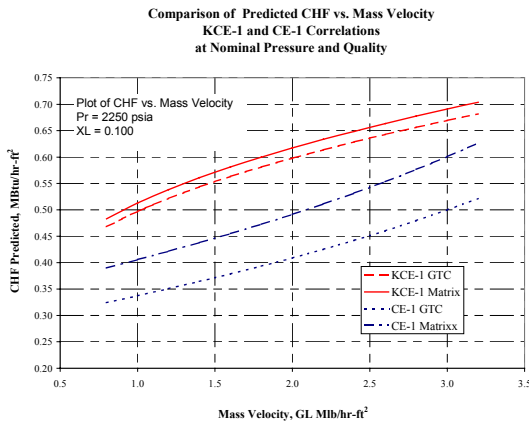


Figure 14 Predicted CHF vs. Mass Velocity at Nominal Pressure & Quality

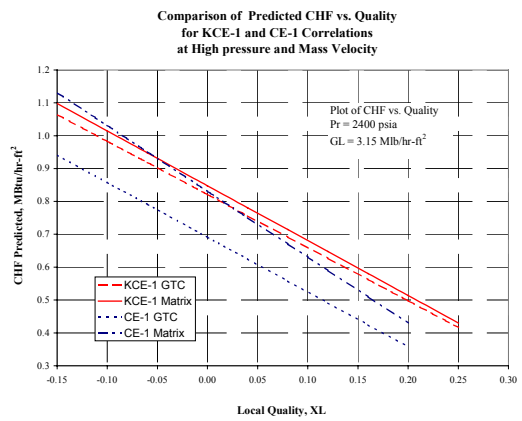


Figure 15 Predicted CHF vs. Quality at High Pressure & Mass Velocity

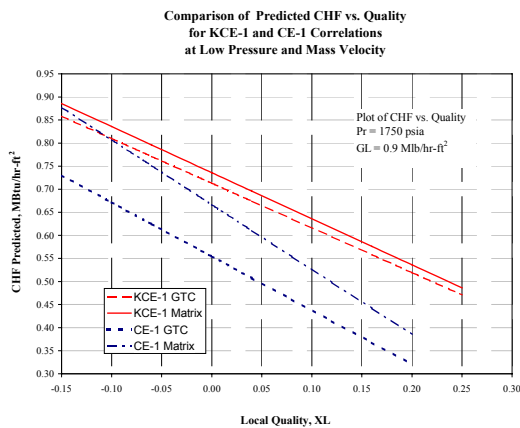


Figure 16 Predicted CHF vs. Quality at Low Pressure & Mass Velocity

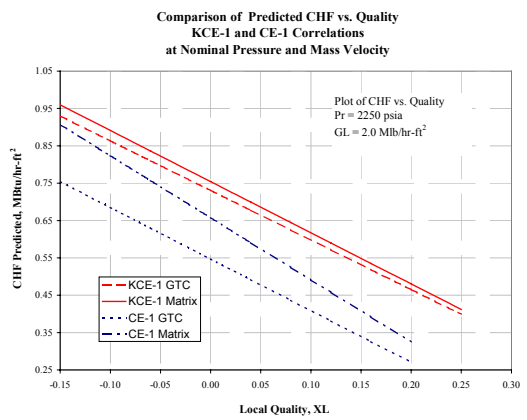


Figure 17 Predicted CHF vs. Quality at Nominal Pressure & Mass Velocity